Observation of Adducts in the Reaction of Cl Atoms with XCH_2I (X = H, CH_3, Cl, Br, I) Using Cavity Ring-Down Spectroscopy

Shinichi Enami, Satoshi Hashimoto, and Masahiro Kawasaki*

Department of Molecular Engineering and Graduate School of Global Environmental Studies, Kyoto University, Kyoto 615-8510, Japan

Yukio Nakano and Takashi Ishiwata

Faculty of Information Sciences, Hiroshima City University, Hiroshima 731-3194, Japan

Kenichi Tonokura

Environmental Science Center, The University of Tokyo, Tokyo 113-0033, Japan

Timothy J. Wallington

Scientific Research Laboratories, Ford Motor Company, Dearborn, Michigan 48121-2053

Received: June 21, 2004; In Final Form: September 29, 2004

The reactions of Cl atoms with XCH_2I (X = H, CH_3, Cl, Br, I) have been studied using cavity ring-down spectroscopy in 25−125 Torr total pressure of N_2 diluent at 250 K. Formation of the XCH_2I−Cl adduct is the dominant channel in all reactions. The visible absorption spectrum of the XCH_2I−Cl adduct was recorded at 405−632 nm. Absorption cross-sections at 435 nm are as follows (in units of 10^{-18} cm^2 $molecule^{-1}$): 12 for CH_3I, 21 for CH_3CH_2I, 3.7 for CH_2ICl, 7.1 for CH_2IBr, and 3.7 for CH_2I_2. Rate constants for the reaction of Cl with CH_3I were determined from rise profiles of the CH_3I−Cl adduct. $k(Cl + CH_3I)$ increases from $(0.4 \pm 0.1) \times 10^{-11}$ at 25 Torr to $(2.0 \pm 0.3) \times 10^{-11}$ cm^3 $molecule^{-1}$ s^{-1} at 125 Torr of N_2 diluent. There is no discernible reaction of the CH_3I−Cl adduct with 5−10 Torr of O_2. Evidence for the formation of an adduct following the reaction of Cl atoms with CF_3I and CH_3Br was sought but not found. Absorption attributable to the formation of the XCH_2I−Cl adduct following the reaction of Cl atoms with XCH_2I (X = H, CH_3, Br, I) was measured as a function of temperature over the range 250−320 K.

1. Introduction

The atmospheric chemistry of iodine-containing compounds is a topic of current interest.[1] Iodinated source gases (CH_3I, CH_2I_2, CH_2BrI, CH_2ClI) in the atmosphere are easily photodissociated in the near-UV region.[2] Iodine in its various forms is rapidly converted to iodine atoms. Iodine chemistry may influence tropospheric HO_2/OH and NO_2/NO concentration ratios and hence the oxidizing capacity of the atmosphere.[3] Thus, iodine chemistry may play an important role in the oxidation of dimethyl sulfide and destruction of ozone in the marine boundary layer.[4,5]

CH_3I is the most abundant iodine-containing species in the air and the main source of active iodine compounds.[1,6] Although its major fate in the marine boundary layer is photodissociation, reactions with OH radicals and Cl atoms together account for about 10% of the loss of CH_3I in the troposphere. Cl atoms are produced from sea salt aerosols in the marine boundary layer.[7] Night-time observations of Cl_2 concentrations at a coastal site during onshore wind flow conditions were reported by Spicer et al.[8] The measured mixing ratios of Cl_2 range from <10 to 150 ppt. The maximum predicted levels of Cl atoms occur shortly after sunrise, peaking at 10^5 cm^{-3}, while the OH mixing ratio is 4×10^5 cm^{-3}.

The reaction of Cl atoms with CH_3I proceeds via two channels: adduct formation and hydrogen atom abstraction

$$CH_3I + Cl + M \rightleftarrows CH_3I{-}Cl + M \quad (1a, -1a)$$

$$CH_3I + Cl \rightarrow CH_2I + HCl \quad (1b)$$

There have been several experimental and theoretical studies of the reaction of CH_3I with Cl atoms.[9−13] At low temperatures ($T \leq 250$ K), the adduct-forming reaction 1a is dominant, and the rate constant for the reaction increases with total pressure.[9] At high temperatures ($T \geq 364$ K) the H-atom abstraction reaction 1b is dominant, and the rate of the reaction is independent of pressure. In the intermediate temperature range of $263 \leq T \leq 309$ K, the reaction displays complex kinetic behavior caused by reversible formation of the adduct via reactions 1a and −1a.[9] In previous work, the formation of the CH_3I−Cl adduct was deduced from observation of the kinetic behavior of Cl atoms. In this paper, we present the first direct measurement of the absorption spectrum of the CH_3I−Cl adduct over the wavelength range 405−532 nm. We report (a) measurements of the visible spectra of the XCH_2I−Cl (X = H, CH_3, Cl, Br, I) adducts and (b) kinetic data for the reaction of Cl atoms with CH_3I at 250 K in 25−125 Torr of N_2 diluent.

* To whom corresponding should be addressed. Fax number: + 81-75-383-2573. E-mail address: kawasaki@moleng.kyoto-u.ac.jp.

10.1021/jp047297y CCC: $30.25
Published on Web 02/05/2005

2. Experimental Section

The cavity ring-down spectroscopy (CRDS) technique was introduced by O'Keefe and Deacon[14] and has been applied widely in spectroscopic and chemical kinetic studies.[15−17] The CRDS apparatus used in the present study has been described elsewhere.[5] The system employs photolysis and probe pulsed lasers. After the photolysis laser beam traverses the glass tube reactor, the probe laser beam is injected nearly collinearly to the axis of the photolysis laser through one of two high-reflectivity mirrors (Research Electro Optics, reflectivity > 0.999 at 405, 435, 488, 532, and 632 nm). Absorption by Cl_2 precludes CRDS measurements below 400 nm. Light leaking from the end mirror was detected by a photomultiplier tube (Hamamatsu Photonics, R212UH) with a fast-response photomultiplier socket assembly (Hamamatsu Photonics, E5815−01, 50-Ohm termination) through suitable narrow band-pass filters. The decay of the light intensity was recorded using a digital oscilloscope (Tektronix, TDL-714L, 8-bit digitizer) and transferred to a personal computer. In the presence of an absorbing species, the light intensity within the cavity is given by the expression

$$I(t) = I_0 \exp(-t/\tau) = I_0 \exp(-t/\tau_0 - \sigma n c L_R t/L_C) \quad (2)$$

where I_0 and $I(t)$ are the light intensities at time 0 and t, τ_0 is the cavity ring-down time without photolysis laser light, L_R is the length of the reaction region (0.46 m), L_C is the cavity length (1.04 m), τ is the cavity ring-down time with photolysis laser light, c is the velocity of light, and n and σ are the concentration and absorption cross-sections of the absorbing species.

The 355-nm output of a Nd^{3+}:YAG laser was used to dissociate Cl_2 to generate Cl atoms. The laser power was measured in each experiment and was typically 20 mJ/pulse. Shot-to-shot fluctuation of the laser power was less than 10%. Absorption by the CH_3I-Cl adduct was monitored with a dye laser (Lambda Physik, SCANMATE, spectral resolution < 0.01 nm). The absorption profile was measured typically between 5 and 85 μs after the photolysis laser pulse for kinetic measurements. A large excess of CH_3I, $10^{15}-10^{16}$ molecule cm^{-3}, ensured that loss of Cl atoms, and formation of products, followed pseudo-first-order reaction conditions.

The reaction cell consisted of a Pyrex glass tube (21 mm i.d.). The temperature of the gas flow region was controlled over $T = 218-298$ K. Experiments below 240 K were difficult to conduct because of low vapor pressure of the parent compounds (except CF_3I and CH_3Br). The difference between the temperature of the sample gas at the entrance and exit of the flow region was <1 K. The total flow rate was adjusted so that the gas in the cell was replaced completely within the 0.5-s time interval between photolysis laser pulses.

To estimate the initial concentration of the Cl atoms, $[Cl]_0$, the production of ClO at 273 K was measured at 266 nm using $Cl_2/O_3/O_2$ mixtures with photolysis of Cl_2 at 355 nm and $[Cl_2] = (1-10) \times 10^{15}$ molecule cm^{-3}.

$$Cl + O_3 \rightarrow ClO + O_2 \quad (3)$$

O_3 was produced by irradiating an oxygen gas flow (slightly higher than 760 Torr) with a low-pressure Hg lamp (Hamamatsu Photonics, L937−02). $[Cl]_0$ was $(1-10) \times 10^{12}$ molecule cm^{-3} at 273 K. Formation of ClOO is negligible at 273 K.[18] The initial chlorine atom concentrations, $[Cl]_0$, in experiments at 250 K were estimated from the calibration at 273 K and literature data for the temperature dependence of the Cl_2 absorption cross-sections.[19]

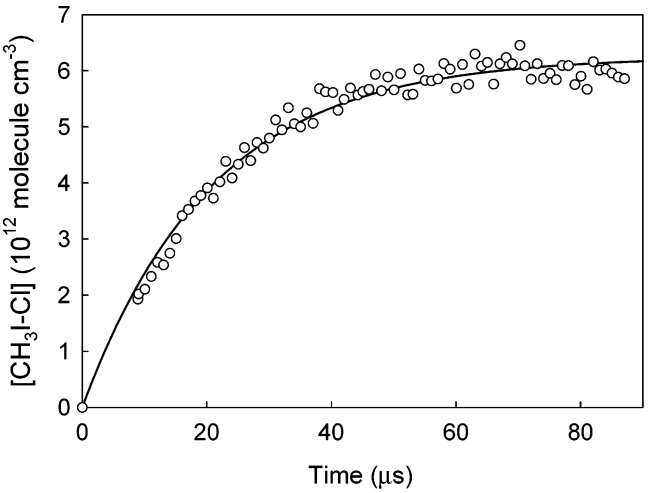

Figure 1. Typical rise profile of the CH_3I-Cl adduct monitored at 435 nm for an experiment conducted in 100 Torr N_2 diluent at 250 K with $[CH_3I] = 1.8 \times 10^{15}$ and $[Cl_2] = 3.3 \times 10^{15}$ molecule cm^{-3}. Adduct concentrations were calculated using $\sigma(CH_3I-Cl) = 1.2 \times 10^{-17}$ cm^2 $molecule^{-1}$. See text for details. The smooth curve is a fit of eq 7 to the data.

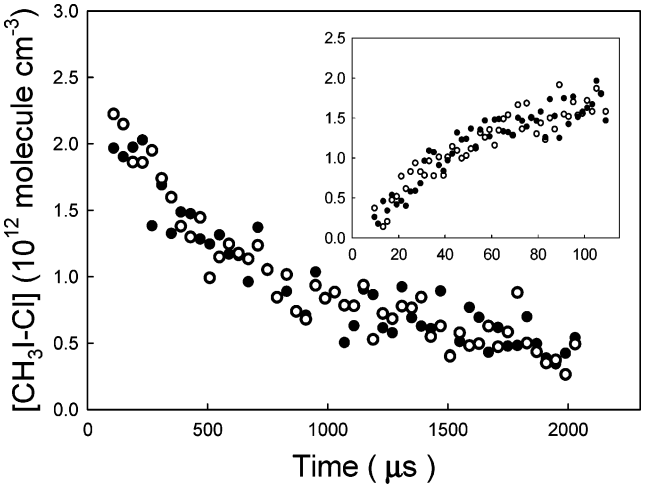

Figure 2. Decay and rise profiles of the CH_3I-Cl adduct at 250 K in either 100 Torr of N_2 (filled symbols) or 90 Torr N_2 and 10 Torr O_2 (open symbols) diluent.

All reagents were obtained from commercial sources. CH_3I (99.5%), CH_2ClI (>97%), CH_2BrI (>98.4%), and CH_2I_2 (>98%) were obtained from Sigma Aldrich. CH_3CH_2I (>99%) and CH_3Br (>99%) were obtained from Tokyo Kasei Kogyo. CH_3I, CH_2ClI, CH_2BrI, CH_2I_2, CH_3Br, and CH_3CH_2I were subjected to freeze−pump−thaw cycling before use. Cl_2 (high purity, Sumitomo Seika), CF_3I (>97%, Lancaster), N_2 (99.999%, Teisan), and O_2 (>99.995%, Teisan) were used without further purification.

3. Results

3.1. Adduct Formation. As described already, the reaction of Cl atoms with CH_3I proceeds via two channels: 1a and 1b. Absorption at 405−532 nm was observed following the UV irradiation of $CH_3I/Cl_2/N_2$ mixtures. Figure 1 shows a typical rise profile of this absorption in 100 Torr total pressure of N_2 diluent at 250 K. As shown in Figure 2, addition of 5 or 10 Torr of O_2 had no discernible effect on either the rise or decay time profiles. These results show that the observed absorption is not attributable to the CH_2I radical produced via the abstraction reaction 1b, because this radical is consumed

rapidly by reaction with O_2.[20]

$$CH_2I + O_2 \rightarrow IO + HCHO \quad (4)$$

According to our previous work on the reaction of CH_2I with O_2 at room temperature, IO radicals are produced in reaction 4.[20] In the present experiments, the structured (3,0) band of IO radicals at 435.63 nm was not observed at 250 K, while it was observed at higher temperatures. These results indicate that for temperatures below 250 K the hydrogen abstraction path 1b is negligible, while above 250 K, its contribution becomes appreciable.

The formation of ICl might contribute to absorption in the probing wavelength region and complicate the present analysis.

$$CH_3I + Cl \rightarrow CH_3 + ICl \quad (1c)$$

However, reaction 1c is endothermic by 28.5 kJ mol^{-1},[21,22] and hence, ICl is not expected to be a significant product of reaction 1. In agreement with the previous work of Ayhens et al.,[9] we conclude that under the present experimental conditions (250 K, 100 Torr N_2 diluent) the reaction of Cl atoms with CH_3I proceeds largely, if not exclusively, via adduct formation. Hence, absorption observed at 400−532 nm following the UV irradiation of $CH_3I/Cl_2/N_2$ mixtures is attributable to the CH_3I-Cl adduct.

3.2. Visible Absorption Spectrum of the CH_3I-Cl Adduct. Absorption cross-sections of the CH_3I-Cl adduct were determined using the following equation

$$1/\tau - 1/\tau_0 = [CH_3I-Cl]\sigma c L_R/L_C \quad (5)$$

where τ is the ring-down time in the presence of the CH_3I-Cl adduct. As discussed in the previous section, the results from Ayhens et al.[9] and the present work show that, at 250 K in the presence of 100 Torr of N_2 diluent, the CH_3I-Cl adduct is essentially the sole product of reaction 1. Decomposition of the CH_3I-Cl adduct occurs slowly at 250 K, $k_{-1a} = 87$ s^{-1},[9] and is not significant over the experimental time scales employed in the present experiments. Cl atoms are lost by reaction with CH_3I and diffusion out of the detection region. For the concentrations of CH_3I employed in the present experiments, $[CH_3I] = 10^{15}-10^{16}$ molecule cm^{-3}, reaction 1 dominates the loss of Cl atoms, and the maximum concentration of CH_3I-Cl can be equated to $[Cl]_0$.

$$[CH_3I-Cl]_{max} = [Cl]_0 \quad (6)$$

The absorption spectrum of the CH_3I-Cl adduct was measured in 0.05-nm steps over the wavelength ranges 434−437 and 485−489 nm. There was no discernible structure in the spectrum. Measured absorption cross-sections at 405, 435, 488, and 532 nm are shown in Figure 3 and Table 1. Allowing for fluctuation of laser power, uncertainties in pressure and mass measurements, and diffusion loss of the adduct, we estimate that the absorption cross-sections given in Figure 3 are accurate to within ±19%. The spectrum for the CH_3I-Cl adduct measured herein is consistent with the charge-transfer (CT) absorption bands calculated by Ayhens et al.[9]

3.3. Adduct Formation in Reactions of Cl Atoms with CH_3CH_2I, CH_2ClI, CH_2BrI, and CH_2I_2. The absorption spectra of the adducts of Cl atoms with CH_3CH_2I, CH_2ClI, CH_2BrI, and CH_2I_2 were also observed at 405−532 nm at 250 K and 100 Torr of N_2 diluent. The absorption cross-sections are shown in Figure 3 and Table 1. The reaction of the $CH_2BrI-Cl$ adduct with O_2 was investigated by adding 5 or 10 Torr of

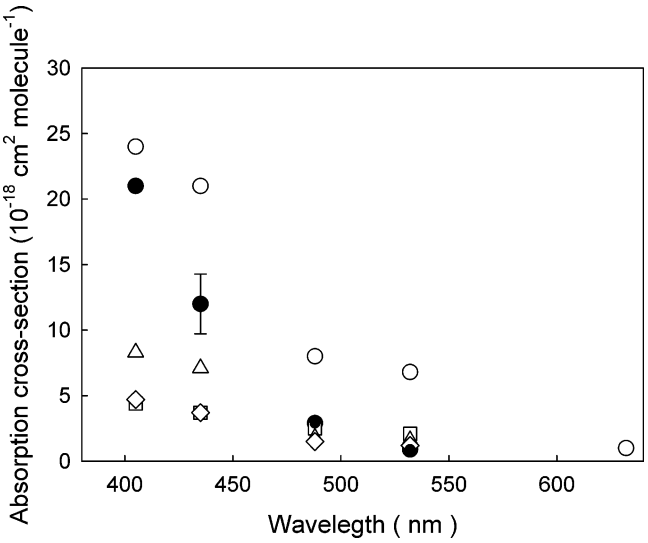

Figure 3. Absorption spectra of XCH_2I-Cl adducts. X = H, closed circles; Cl, triangles; Br, squares; I, diamonds; and CH_3, open circles. Error bars are 19% for all points.

TABLE 1: Absorption Cross-Sections of Cl Adducts with CH_3I, CH_3CH_2I, CH_2ClI, CH_2BrI, and CH_2I_2 at 250 K

wavelength (nm)	absorption cross-section[a] (10^{-18} cm^2 molecule^{-1})				
	CH_3I-Cl	CH_3CH_2I-Cl	$CH_2ClI-Cl$	$CH_2BrI-Cl$	CH_2I_2-Cl
405	21	24	4.4	8.3	4.7
435	12	21	3.7	7.1	3.7
488	2.9	8.0	2.5	1.8	1.5
532	0.9	6.8	2.1	1.6	1.2
632		1.0			

[a] Error bars are 19%.

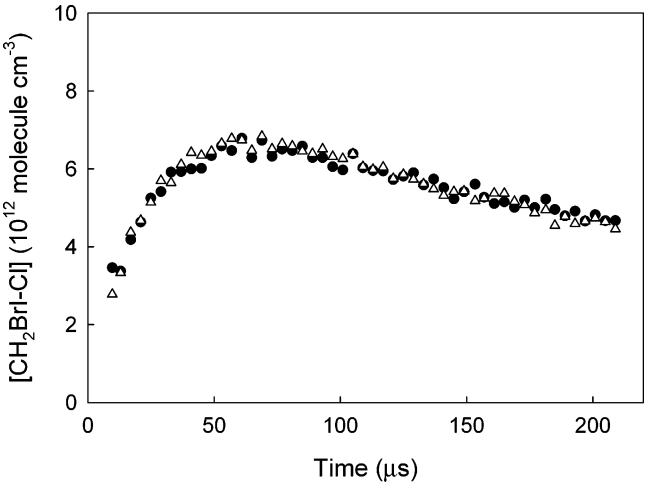

Figure 4. Time profiles of the $CH_2BrI-Cl$ adduct at 250 K in either 100 Torr of N_2 (filled circles) or 90 Torr N_2 and 10 Torr O_2 (open triangles) diluent.

O_2 to the reaction mixtures. As shown in Figure 4, there was no discernible change in either the rise or decay time-profiles in the presence of O_2. We conclude that the spectra are attributable to adducts and not to alkyl radicals (which react rapidly with O_2) and that there is no discernible reaction of the adducts with O_2. The spectra were calibrated by assuming that at 250 K the adduct is the sole reaction product. As seen from Table 1, CH_3CH_2I-Cl has the largest cross-section, about twice that of CH_3I-Cl. The cross-sections for $CH_2ClI-Cl$, $CH_2BrI-Cl$, and CH_2I_2-Cl are indistinguishable.

Experiments were conducted for CF_3I and CH_3Br at temperatures as low as 218 K in 100 Torr of N_2 diluent in an attempt

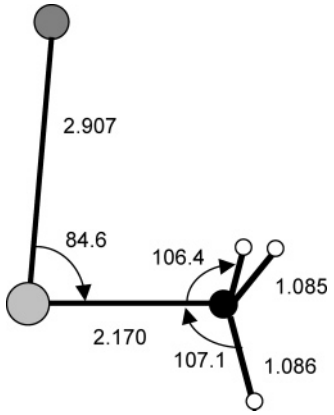

Figure 5. Optimized structure of the CH_3I-Cl adduct.

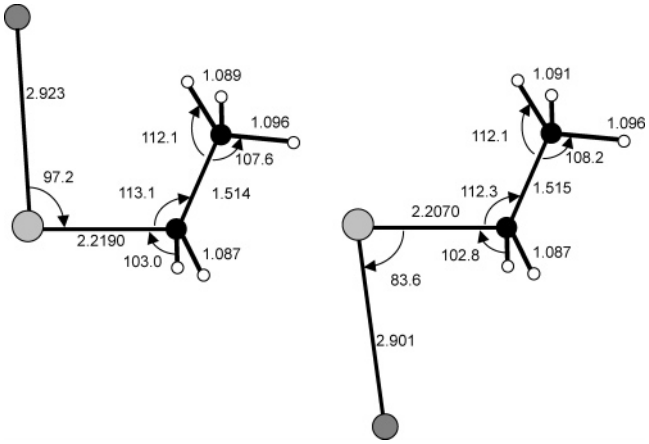

Figure 6. Optimized structures of *cis*- and *trans*-C_2H_5I-Cl adducts. The trans isomer is 3.8 kJ mol^{-1} more stable than the cis isomer.

to observe evidence for adduct formation in the form of absorption at 405 and 435 nm. No such evidence was observed, and we conclude that adduct formation is not significant for the reaction of Cl atoms with CF_3I and CH_3Br at temperatures of >218 K. This conclusion is consistent with work by Piety et al.[23] suggesting that CH_3Br reacts with Cl to form CH_2Br + HCl at 250 K and by Kaiser et al. suggesting that CF_3I reacts with Cl to form CF_3 + ICl at 271−363 K.[24]

3.4. Theoretical Calculation of Electronic Excitation Energies of CH_3I-Cl and C_2H_5I-Cl Adducts. All calculations were carried out with the *Gaussian 03* Revision B.04 program packages.[25] The equilibrium geometries of the ground state of the CH_3I-Cl and CH_3CH_2I-Cl adducts were optimized employing a hybrid density functional theory B3LYP, based on Becke's three-grid integration[26−28] and exchange functional and the correction functional of Lee, Yang, and Parr.[29] A 6-311++G(d,p) basis set was used for carbon and hydrogen, while a 6-3llG(d,p) basis set was used for iodine and chlorine. Electronic transitions of the adducts were investigated employing time-dependent density functional theory (TD-DFT) calculations.[30]

The calculations were based on the $^2A'$ ground-state equilibrium.[31] C_s molecular symmetry was assumed for the equilibrium geometry of the ground state that is shown in Figures 5 and 6. There are cis and trans isomers for CH_3CH_2I-Cl. The present calculations predicted that the trans isomer is 3.8 kJ mol^{-1} more stable than the cis isomer. Vibrational analyses showed an imaginary frequency for the cis isomer but no imaginary frequency for the trans isomer. The theoretically determined I−Cl bond strengths for CH_3I-Cl and CH_3CH_2I-Cl are 59.0 and 61.7 kJ mol^{-1}, respectively. The value for

TABLE 2: Electronic Transition Energies and Oscillator Strengths of CH_3I-Cl and C_2H_5I-Cl

state	energy (eV)	wavelength (nm)	oscillator strength
	CH_3I-Cl		
$1^2A'$	0		
$1^2A''$	1.1255	1101.6	0.0002
$2^2A'$	1.2778	970.33	0.0003
$2^2A''$	2.2693	546.35	0
$3^2A'$	3.6539	339.32	0.1753
$4^2A'$	4.0378	307.06	0.1750
$3^2A''$	4.2250	293.46	0
$4^2A''$	4.6975	263.94	0
$5^2A'$	4.8237	257.03	0.0012
$6^2A'$	4.9350	251.23	0.0112
	trans-CH_3CH_2I-Cl		
$1^2A'$	0		
$1^2A''$	1.1500	1078.09	0.0002
$2^2A'$	1.3124	944.73	0.0003
$2^2A''$	2.2364	554.39	0
$3^2A'$	3.6241	342.11	0.1589
$4^2A'$	3.9913	310.64	0.1675
$5^2A'$	4.1805	296.58	0.0333
$3^2A''$	4.1894	295.95	0
$4^2A''$	4.6582	266.17	0
$6^2A'$	4.8829	253.91	0.0077

CH_3I-Cl is in good agreement with the previously reported theoretical calculation, 59.3 kJ mol^{-1}, by Ayhens et al.[9]

For CH_3I-Cl, photoabsorption appears at 339.32 nm with an oscillator strength $f = 0.1753$ and at 307.06 nm with $f = 0.1750$. This oscillator strength corresponds to the absorption cross-section of 1.8×10^{-17} cm^2 $molecule^{-1}$ when the absorption spectrum is assumed to have a Gaussian shape with a full-width at half-maximum of 100 nm. These transitions are assigned to a $\sigma-\sigma^*$ transition localized on the I−Cl bond and a $\sigma^*-\sigma^*$ transition from the σ^* orbital on the I−Cl bond to the σ^* orbital on the I−Cl bond, respectively. Similarly, for CH_3CH_2I-Cl, absorption appears at 342.11 nm with $f = 0.1589$ and 310.64 nm with $f = 0.1675$. Detailed results are listed in Table 2. The experimental observations (see Figure 3) are attributable to the red wing of these transitions.

3.5. Measurement of $k(CH_3I-Cl)$ at 250 K. The absorption of the CH_3I-Cl adduct was monitored at 435 nm. In the presence of a large excess of CH_3I over Cl atoms, the rise profile follows pseudo-first-order kinetics. For the experimental conditions used in the present work, at 250 K the forward reaction 1a is dominant and the reverse reaction (−1a) is sufficiently slow that it can be neglected ($k_{-1a} = 87$ s^{-1}).[9] The rise of absorption at 435 nm provides kinetic information regarding the overall rate constant for reaction 1 (i.e., $k_{1a} + k_{1b}$). However, as discussed in section 3.1, under the present experimental conditions (250 K in 100 Torr of N_2), reaction channel 1b is of minor importance and hence $k_1 \approx k_{1a}$. The formation of the CH_3I-Cl adduct may be analyzed using the following equations

$$[CH_3I-Cl]_t = [Cl]_0\{1 - \exp(-k't)\} \quad (7)$$

$$k' = k_{1a}[CH_3I] + k_d \quad (8)$$

where $[CH_3I-Cl]_t$ is the concentration of CH_3I-Cl at time t. k_{1a} and k' are the second-order and pseudo-first-order rate constants for reaction 1a, respectively. k_d is the rate constant for diffusion from the observation region, which is experimentally obtained as the intercept at $[CH_3I] = 0$. Figure 1 shows a typical rise profile of the CH_3I-Cl adduct at 250 K with $[CH_3I] = 1.8 \times 10^{15}$ molecule cm^{-3}. The smooth curve is a fit of eq 7 to the data. The concentration of CH_3I-Cl was determined

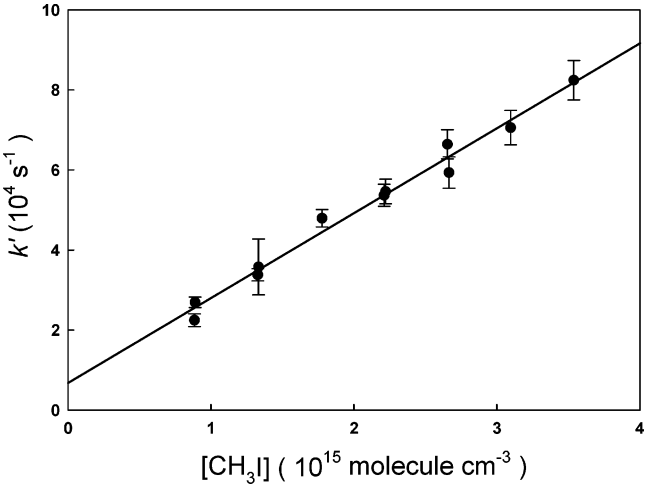

Figure 7. Second-order plot for reaction of Cl with CH_3I in 100 Torr N_2 diluent at 250 K.

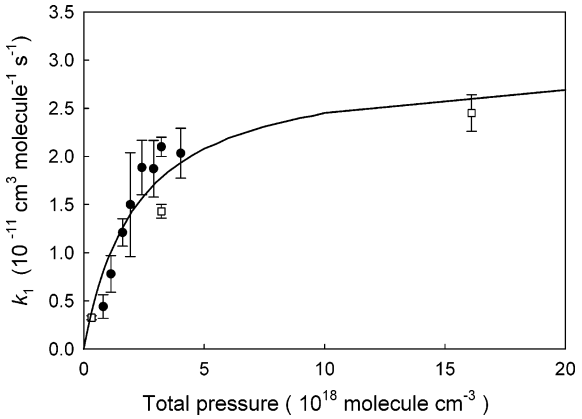

Figure 8. Rate constants of the reaction of Cl with CH_3I as a function of total pressure of N_2 diluent at 250 K. Open squares are taken from Ayhens et al.[9] The solid curve is the fit of eq 9 to the data.

using the absorption cross-section given in Table 1. Figure 7 shows a plot of k' versus $[CH_3I]$ at 250 K in 100 Torr total pressure of N_2 diluent. Linear least-squares analysis of the data in Figure 7 gives the second-order rate constant $k_{1a} = (2.1 \pm 0.1) \times 10^{-11}$ cm^3 molecule^{-1} s^{-1}. The *y*-axis intercept in Figure 7 is $k_d = 6800 \pm 2000$ s^{-1} and is consistent with our previous experimental results.[32]

Figure 8 shows a plot of k_{1a} versus total pressure. The rate constant increases from $(0.4 \pm 0.1) \times 10^{-11}$ to $(2.0 \pm 0.3) \times 10^{-11}$ cm^3 molecule^{-1} s^{-1} as the total pressure of the N_2 diluent was increased from 25 to 125 Torr. These results are typical for a three-body reaction and support the formation of the CH_3I-Cl adduct. The curve in Figure 8 is a fit of the equation for the simple hard-collision mechanism to the combined data.

$$k_{1a} = \frac{k_{1a}^{low}[M]}{1 + (k_{1a}^{low}[M]/k_{1a}^{high})} \qquad (9)$$

The best fit is achieved with $k_{1a}^{low} = (1.4 \pm 0.3) \times 10^{-29}$ cm^6 molecule^{-2} s^{-1} and $k_{1a}^{high} = (3.0 \pm 0.4) \times 10^{-11}$ cm^3 molecule^{-1} s^{-1}. More data at high pressure are needed to more accurately define the high-pressure limiting rate constant for this reaction.

3.6. Temperature Dependence of CH_3I-Cl Adduct Formation. The observed absorbance at 435 nm following flash photolysis of $CH_3I/Cl_2/N_2$ mixtures was measured at the maximum concentration (typically, $t = 80$ μs) as a function of temperature over the range 250−325 K in 100 Torr N_2 diluent. The absorption was normalized to that observed at 250 K and plotted versus temperature in Figure 9. As seen from Figure 9, the absorption attributable to the formation of CH_3I-Cl decreases almost linearly with increasing temperature. The ratios of absorbance at 435 and 488 nm were measured at three different temperatures, 250, 273, and 318 K and were σ(488 nm)/σ(435 nm) = 0.24 ± 0.04, 0.27 ± 0.04, and 0.27 ± 0.04, respectively. The shape of the absorption spectrum does not change over the temperature range 250−318 K. We conclude that the decrease in absorbance at 435 nm with increasing temperature shown in Figure 9 reflects a decreasing yield of the CH_3I-Cl adduct with increasing temperature.

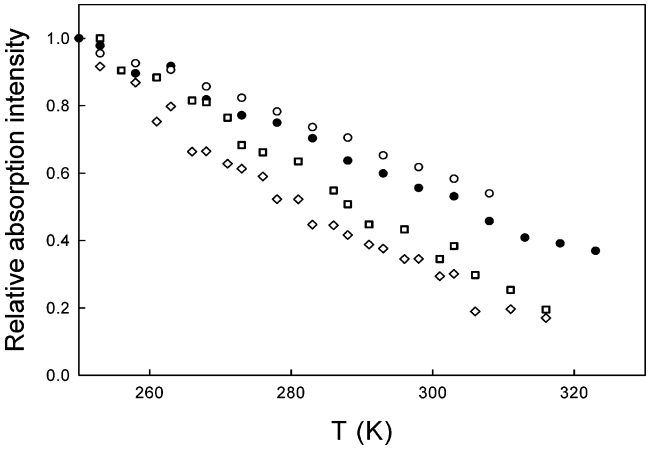

Figure 9. Absorbance at 435 nm (relative to that at 250 K) for XCH_2I-Cl adducts as a function of temperature; X = H, closed circles; Br, squares; I, diamonds; and CH_3, open circles. All experiments were performed in 100 Torr of N_2 diluent.

Linear extrapolation of the CH_3I-Cl data in Figure 9 gives an *x*-axis intercept, 356 ± 10 K, at which there will be no appreciable adduct formation. This result is consistent with the previous report by Ayhens et al.[9] that adduct formation is not significant at 364 K in 100 Torr N_2 diluent. In the present experiment, the observed decrease in concentration of CH_3I-Cl above 250 K, $\Delta[CH_3I-Cl]_{obs}$, is attributable to increased rates of reactions −1a and 1b as temperature is increased. To provide insight into the relative importance of these factors and a more quantitative comparison of our results with those reported by Ayhens et al.,[9] a modeling exercise was undertaken. The model consisted of reactions 1a, −1a, and 1b with rate constants k_{1a}, k_{-1a}, and k_{1b} reported by Ayhens et al.[9] in 100 Torr N_2 diluent. The loss of Cl atoms via diffusion from the viewing zone was included in the model. The IBM *Chemical Kinetics Simulator* program was used to calculate the maximum concentration (at typically $t = 80$ μs) of the CH_3I-Cl adduct for "experiments" conducted at different temperatures. In the calculations, uncertainties in the diffusion constant, $k_d = 6800 \pm 2000$ s^{-1}, were taken into account, but those of the reported rate constants were not. The squares in Figure 10 show the results of the modeling exercise.

The solid curve in Figure 10 is a fit through the model results to aid visual inspection of the data trend. The magnitude of uncertainties in the experimental data is indicated by the error bars for the data points (circles) at 279 and 318 K, while uncertainties in the model results are indicated for the data points (squares) at 283 and 323 K. As seen from Figure 10, the experimental observations in the present work are, within the combined uncertainties, consistent with those predicted using the kinetic data reported by Ayhens et al.[9] Examples of rate constants used in the calculation are the following: $k_{1a} = 1.38$

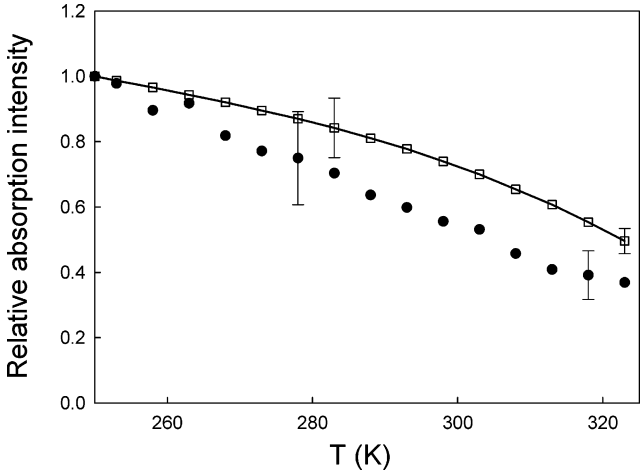

Figure 10. Temperature dependence of the relative absorbance of CH_3I-Cl at 435 nm; circles are experimental data measured herein, squares and solid curve were calculated from the kinetic data reported by Ayhens et al.[9] (see text for details).

$\times 10^{-11}$ cm^3 molecule^{-1} s^{-1}, $k_{-1a} = 87.6$ s^{-1}, $k_{1b} = 3.85 \times 10^{-13}$ cm^3 molecule^{-1} s^{-1} at 250 K, and $k_{1a} = 6.87 \times 10^{-12}$ cm^3 molecule^{-1} s^{-1}, $k_{-1a} = 1.42 \times 10^4$ s^{-1}, $k_{1b} = 1.13 \times 10^{-12}$ cm^3 molecule^{-1} s^{-1} at 323 K. The branching ratio for adduct formation $k_{1a}/(k_{1a} + k_{1b})$ decreases from 0.97 to 0.86 over the temperature range 250−323 K. In 100 Torr of N_2 diluent at 323 K, the pseudo-first-order rate of adduct formation via reaction 1a is 1.27×10^4 s^{-1}, while decomposition of the adduct via reaction −1a occurs at a rate of 1.42×10^4 s^{-1}. Unimolecular decomposition of the CH_3I-Cl adduct via reaction −1a is the main reason for the observed temperature dependence shown in Figure 10.

3.7. Temperature Dependence of Adduct Formation in Reactions of Cl with CH_3CH_2I, CH_2BrI, and CH_2I_2. Similarly to the case of the CH_3I-Cl adduct, assuming that the absorption cross-section of the XCH_2I-Cl (X = CH_3, Br, and I) adducts at 435 nm do not change significantly over the temperature range studied, the decrease in absorption with temperature is attributable to an increase in the rates of both the abstraction reaction and the back reaction. The *x*-intercepts of linear extrapolation in Figure 9 are 377 ± 8, 333 ± 11, and 315 ± 12 K for XCH_2I-Cl (X = CH_3, Br, and I), respectively. At these decomposition temperatures, no discernible adduct formation is expected.

4. Discussion

It has been established previously that adduct formation plays an important role in the reaction of F atoms with CHF_2Br, CH_2BrCl, and CH_3Br.[34−36] CHF_2Br-F, $CH_2BrCl-F$, and CH_3Br-F adducts display strong UV absorption with a maximum absorption cross-section of approximately 2×10^{-17} cm^2 molecule^{-1} at 290 nm. The reaction of Cl + CH_2ClI has a small negative activation energy, suggesting the importance of long-range attractive forces in its reaction dynamics.[21] Wine and co-workers have reported that reactions of Cl atoms with CH_3I, CH_3Br, CF_3CH_2I, and CD_3CD_2I proceed via two channels: adduct formation and direct hydrogen abstraction.[9,23] We report herein the formation of adducts in the reactions of Cl atoms with CH_3I, CH_2ClI, CH_2IBr, CH_2I_2, and C_2H_5I. It appears that the formation of short-lived adducts is a common facet of the reactions of F and Cl atoms with bromo- and iodo-compounds.

Ab initio calculations by Piety et al. predict an adduct bond strength of 59.l kJ mol^{-1} for CD_3CD_2I-Cl.[23] Kambanis et al. reported the existence of stable adducts of Cl atoms with HI, CH_3I, and CH_3OCH_2I at 298 K with bond strengths of 31.1, 52.4, and 51.3 kJ mol^{-1}, respectively.[10] In the present work, CH_3I-Cl and C_2H_5I-Cl adducts are calculated to have bond strengths of 59.0 and 61.7 kJ mol^{-1} and are characterized by decomposition temperatures (*x*-axis intercepts in Figure 9) of 356 and 377 K, respectively. The decomposition temperatures of $CH_2BrI-Cl$ and CH_2I_2-Cl adducts are 333 and 315 K, respectively, indicating lower bond strengths than for the C_2H_5I-Cl and CH_3I-Cl adducts.

Absorption cross-sections of XCH_2I-Cl adducts at 405 and 435 nm decrease in the order $C_2H_5I > CH_3I > CH_2BrI \approx CH_2I_2 \approx CH_2ClI$. No adduct formation was observed in the reaction of Cl atoms with CF_3I and CH_3Br. CT complex formation offers a qualitative explanation of the observed trends, because the ionization potentials (I_P) of the parent compounds are as follows: $I_P(C_2H_5I) = 9.4$ eV, $I_P(CH_3I) = 9.5$ eV, $I_P(CH_2I_2) = 9.5$ eV, $I_P(CH_2BrI) \approx 9.6$ eV, $I_P(CH_2ClI) = 9.7$ eV, $I_P(CF_3I) = 10.3$ eV, and $I_P(CH_3Br) = 10.5$ eV.[37−40]

Piety et al. reported that the reaction of Cl atoms with CH_3Br proceeds with a rate constant which is independent of total pressure and that the dominant reaction pathway at $T > 213$ K is hydrogen transfer and not adduct formation.[23] Consistent with the findings of Piety et al., no evidence was observed in the present work for the formation of a CH_3Br-Cl adduct at temperatures of >218 K.

The present work improves our understanding of the kinetics and mechanisms of the reaction of Cl atoms with halogenated methanes in three respects. First, we report the first measurements of the visible spectra of the XCH_2I-Cl (X = H, CH_3, Cl, Br, I) adducts. The experimentally observed spectra are supported by our theoretical calculations. Second, we confirm the literature kinetic data for the reaction of Cl atoms with CH_3I at 250 K.[9] Third, we confirm that at temperatures greater than 218 K adduct formation does not play a significant role in the reaction of Cl atoms with CH_3Br and CF_3I.

Acknowledgment. The authors are grateful to Junya Ueda and Yuki Ito for their help in experiments. T.I. is grateful to a grant from Hiroshima City University for Special Academic Research (General Studies). This work is partly supported by a Grant-in-Aid from the Ministry of Education, Japan in the priority research field "Radical Chain Reactions" and by a grant from the 21st Century COE project of Kyoto University.

References and Notes

(1) Carpenter, L. J. *Chem. Rev.* **2003**, *103*, 49.
(2) Brasseur, G. P.; Orlando, J. J.; Tyndall, G. S. *Atmospheric Chemistry and Global Change*; Oxford University Press: New York, NY, 1999.
(3) Davis, D.; Crawford, J.; Liu, S.; McKeen, S.; Bandy, A.; Thornton, D.; Rowland, F.; Blake, D. *J. Geophys. Res.* **1996**, *101*, 2135.
(4) Kanaya, Y.; Akimoto, H. *Chem. Rec.* **2002**, *2*, 199.
(5) Nakano, Y.; Enami, S.; Nakamichi, S.; Aloisio, S.; Hashimoto, S.; Kawasaki, M. *J. Phys. Chem. A* **2003**, *107*, 6381.
(6) Yokouchi, Y.; Mukai, H.; Yamamoto, H.; Otsuki, A.; Saitoh, C.; Nojiri, Y. *J. Geophys. Res.* **1997**, *102*, 8805.
(7) McFiggans, G.; Cox, R. A.; Mossinger, J. C.; Allan, B. J.; Plane, J. M. C. *J. Geophys. Res.* **2002**, *107*, 15.
(8) Spicer, C. W.; Chapman, E. G.; Finlayson-Pitts, B. J.; Plastridge, R. A.; Hubbe, J. M.; Fast, J. D.; Berkowitz, C. M. *Nature* **1998**, *394*, 353.
(9) Ayhens, Y. V.; Nicovich, J. M.; McKee, M. L.; Wine, P. H. *J. Phys. Chem. A* **1997**, *101*, 9382.
(10) Kambanis, K. G.; Lazarou, Y. G.; Papagiannakopoulos, P. *Chem. Phys. Lett.* **1997**, *268*, 498.
(11) Bilde, M.; Wallington, T. J. *J. Phys. Chem. A* **1998**, *102*, 1550.
(12) Cotter, E. S. N.; Booth, N. J.; Canosa-Mas, C. E.; Gray, D. J.; Shallcross, D. E.; Wayne, R. P. *Phys. Chem. Chem. Phys.* **2001**, *3*, 402.
(13) Lazarou, Y. G.; Kambanis, K. G.; Papagiannakopoulos, P. *Chem. Phys. Lett.* **1997**, *271*, 280.
(14) O'Keefe, A.; Deacon, D. A. G. *Rev. Sci. Instrum.* **1988**, *59*, 2544.

(15) Yu, T.; Lin, M. C. *J. Am. Chem. Soc.* **1993**, *115*, 4371.
(16) Wheeler, M. D.; Newman, S. M.; Orr-Ewing, A. J.; Ashfold, M. N. R. *J. Chem. Soc., Faraday Trans.* **1998**, *94*, 337.
(17) Berden, G.; Peeters, R.; Meijer, G. *Int. Rev. Phys. Chem.* **2000**, *19*, 565.
(18) Suma, K.; Sumiyoshi, Y.; Endo, Y.; Enami, S.; Aloisio, S.; Hashimoto, S.; Kawasaki, M.; Nishida, S.; Matsumi, Y. *J. Phys. Chem. A* **2004**, *108*, 8096.
(19) Sander, S. P.; Friedl, R. R.; Ravishankara, A. R.; Golden, D. M.; Kolb, C. E.; Kurylo, M. J.; Huie, R. E.; Orkin, V. L.; Molina, M. J.; Moortgat, G. K.; Finlayson-Pitts, B. J. *Chemical Kinetics and Photochemical Data for Use in Stratospheric Modeling*; Evaluation 14; Jet Propulsion Laboratory, NASA: California, 2003.
(20) Enami, S.; Ueda, J.; Goto, M.; Nakano, Y.; Aloisio, S.; Hashimoto, S.; Kawasaki, M. *J. Phys. Chem. A* **2004**, *108*, 6347.
(21) Bilde, M.; Sehested, J.; Nielsen, O. J.; Wallington, T. J.; Meagher, R. J.; McIntosh, M. E.; Piety, C. A.; Nicovich, J. M.; Wine, P. H. *J. Phys. Chem. A* **1997**, *101*, 8035.
(22) *NIST Chemistry Webbook*; Standard Reference Database, Vol. 69.
(23) Piety, C. A.; Soller, R.; Nicovich, J. M.; McKee, M. L.; Wine, P. H. *Chem. Phys*. **1998**, *231*, 155.
(24) Kaiser, E. W.; Wallington, T. J.; Hurley, M. D. *Int. J. Chem. Kinet*. **1995**, *27*, 205.
(25) Frisch, M. J.; Trucks, G. W.; Schlegel, H. B.; Scuseria, G. E.; Robb, M. A.; Cheeseman, J. R.; Montgomery, J. A., Jr.; Vreven, T.; Kudin, K. N.; Burant, J. C.; Millam, J. M.; Iyengar, S. S.; Tomasi, J.; Barone, V.; Mennucci, B.; Cossi, M.; Scalmani, G.; Rega, N.; Petersson, G. A.; Nakatsuji, H.; Hada, M.; Ehara, M.; Toyota, K.; Fukuda, R.; Hasegawa, J.; Ishida, M.; Nakajima, T.; Honda, Y.; Kitao, O.; Nakai, H.; Klene, M.; Li, X.; Knox, J. E.; Hratchian, H. P.; Cross, J. B.; Adamo, C.; Jaramillo, J.; Gomperts, R.; Stratmann, R. E.; Yazyev, O.; Austin, A. J.; Cammi, R.; Pomelli, C.; Ochterski, J. W.; Ayala, P. Y.; Morokuma, K.; Voth, G. A.; Salvador, P.; Dannenberg, J. J.; Zakrzewski, V. G.; Dapprich, S.; Daniels, A. D.; Strain, M. C.; Farkas, O.; Malick, D. K.; Rabuck, A. D.; Raghavachari, K.; Foresman, J. B.; Ortiz, J. V.; Cui, Q.; Baboul, A. G.; Clifford, S.; Cioslowski, J.; Stefanov, B. B.; Liu, G.; Liashenko, A.; Piskorz, P.; Komaromi, I.; Martin, R. L.; Fox, D. J.; Keith, T.; Al-Laham, M. A.; Peng, C. Y.; Nanayakkara, A.; Challacombe, M.; Gill, P. M. W.; Johnson, B.; Chen, W.; Wong, M. W.; Gonzalez, C.; Pople, J. A. *Gaussian 03*, revision B.04; Gaussian, Inc.: Pittsburgh, PA, 2003
(26) Becke, A. D. *J. Chem. Phys.* **1993**, *98*, 5648.
(27) Becke, A. D. *J. Chem. Phys.* **1992**, *96*, 2155.
(28) Becke, A. D. *J. Chem. Phys.* **1992**, *97*, 9173.
(29) Lee, C.; Yang, W.; Parr, R. G. *Phys. Rev. B* **1988**, *37*, 785.
(30) Koch, W.; Holthausen, M. C. *A Chemist's Guide to Density Functional Theory*; Wiley-VCH: Weinheim, Germany, 2000.
(31) Hirata, S.; Head-Gordon, M. *Chem. Phys. Lett.* **1999**, *302*, 375.
(32) Enami, S.; Nakano, Y.; Hashimoto, S.; Kawasaki, M.; Aloisio, S.; Francisco, J. *J. Phys. Chem. A* **2004**, *108*, 7785.
(33) Troe, J. *Chem. Rev*. **2003**, *103*, 4565.
(34) Bilde, M.; Sehested, J.; Mogelberg, T. E.; Wallington, T. J.; Nielsen, O. J. *J. Phys. Chem.* **1996**, *100*, 7050.
(35) Bilde, M.; Sehested, J.; Nielsen, O. J.; Wallington, T. J. *J. Phys. Chem. A* **1997**, *101*, 5477.
(36) Sehested, J.; Bilde, M.; Møgelberg, T. E.; Wallington, T. J.; Nielsen, O. J. *J. Phys. Chem*. **1996**, *100*, 10989.
(37) Atkinson, R.; Baulch, D. L.; Cox, R. A.; Hampson, R. F., Jr.; Kerr, J. A.; Rossi, M. J.; Troe, J. *IUPAC Summary of Evaluated Kinetic and Photochemical Data for Atmospheric Chemistry*; Appendix; 2000.
(38) Tian, S. X.; Kishimoto, N.; Ohno, K. *J. Phys. Chem. A* **2003**, *107*, 485.
(39) Since $I_P(CH_2BrI)$ has been not yet known, the value of 9.6 eV is taken as the mean value of $I_P(CH_2ClI)$ and $I_P(CH_2I_2)$.
(40) Mulliken, R. S.; Person, W. B. *Ann. Rev. Phys. Chem*. **1962**, *13*, 107.